Ninth International Conference on Computational Fluid Dynamics (ICCFD9), Istanbul, Turkey, July 11-15, 2016

ICCFD9-xxxx

A SGS Model for LES of Turbulent Buoyant Flows

Ilyas Yilmaz

Department of Mechanical Engineering, Faculty of Engineering,
Istanbul Aydin University, Istanbul 34295, Turkey

Corresponding author: ilyasyilmaz@aydin.edu.tr

Abstract: A novel subgrid-scale (SGS) model for LES of turbulent buoyant flows is proposed. For this purpose, the WALE model is reformulated to take buoyancy effects into account. The proposed model recovers the WALE model for isothermal flows. No scaling is needed near walls. It is applicable to incompressible and compressible turbulent flows with the uniform accuracy and efficiency. Large temperature differences can also be handled without the Oberbeck-Boussinesq (OB) assumption. The buoyancy-modified WALE (BM-WALE) model is applied to the turbulent Rayleigh-Bénard Convection (RBC). The results are successfully compared with the previous experimental and numerical data.

Keywords: Large Eddy Simulation, Subgrid-scale modeling, the WALE model, Buoyancy, Rayleigh-Bénard convection.

1 Introduction

Buoyancy-affected turbulent flows are frequently encountered in both nature and industry. Those effects are usually taken into account via the source term in the governing equations for the resolved flow in Large Eddy Simulation (LES). However, their contribution to turbulent production through unresolved scales obviously requires proper subgrid-scale (SGS) models. This has been an active research area for many years. Lily[1] first addressed to this issue. Then, Eidson[2] formulated the buoyancy contribution into turbulent production and developed a modified version of the Smagorinsky SGS model based on some of the assumptions of turbulent flows. Although this model was used in many studies, Bastiaans et al.[3] and Kimmel and Domaradzki [4] found strong deviations from Direct Numerical Simulation (DNS) results in thermal plume and thermally-driven cavity cases. Peng and Davidson[5] proposed another time scaling to the Eidson model to remedy the problem of having possible non-physical solutions. However, they also reported large discrepancies for both approaches unless the coefficients are determined dynamically. Similar studies on modeling turbulent buoyant flows can also found in the relevant literature. As of today, the problem is still of interest.

The Wall-Adapting Local Eddy-viscosity (WALE) model is an advanced and efficient SGS model successfully applied to various problems in turbulent flows [6]. In this study the well-known WALE model is reformulated to account for buoyancy effects in the unresolved scales in LES. The buoyancy-modified WALE (BM-WALE) model is applied to the turbulent Rayleigh-Bénard Convection (RBC) flow. Results of the proposed approach are presented and discussed in detail.

2 Numerical Method

The base algorithm is a non-dissipative, fully implicit, iterative, pressure-correction solution procedure[7] which conserves kinetic energy and solves the compressible Navier-Stokes equations. A gravitational source

term was added. The set of low-Mach number scaled, non-dimensional governing equations read

$$\frac{\partial \rho}{\partial t} + \frac{\partial (\rho u_j)}{\partial x_j} = 0 \tag{1}$$

$$\frac{\partial (\rho u_i)}{\partial t} + \frac{\partial (\rho u_i u_j)}{\partial x_j} = -\frac{\partial p}{\partial x_i} + \frac{1}{Re}\frac{\partial \tau_{ij}}{\partial x_j} + \frac{1}{Fr^2}\rho g_i \tag{2}$$

$$\begin{aligned} Mr^2 \left[\frac{\partial}{\partial t}\left(p + \frac{\gamma-1}{2}\rho u_i u_i \right) + \frac{\partial}{\partial x_j}\left(\gamma p + \frac{\gamma-1}{2}\rho u_i u_i \right) u_j \right] + \frac{\partial u_j}{\partial x_j} \\ = \frac{(\gamma-1)Mr^2}{Re}\frac{\partial (\tau_{ij} u_i)}{\partial x_j} + \frac{\partial}{\partial x_j}\left(\frac{\mu}{RePr}\frac{\partial T}{\partial x_j} \right) + \frac{Ec}{Fr^2}(\rho u_i g_i) \end{aligned} \tag{3}$$

together with the non-dimensional form of the EOS obtained as $\rho T = \gamma Mr^2 p + 1$.

The discretization is fully implicit and second-order in both space and time. The linear systems arising from discretization are efficiently solved using incomplete LU-preconditioned GMRES.

3 LES Formulation

Employing the box filter and introducing the Favre-weighting, the final form of the non-dimensional LES equations are obtained as follows

$$\frac{\partial \bar{\rho}}{\partial t} + \frac{\partial (\bar{\rho}\tilde{u}_j)}{\partial x_j} = 0 \tag{4}$$

$$\frac{\partial (\bar{\rho}\tilde{u}_i)}{\partial t} + \frac{\partial (\bar{\rho}\tilde{u}_i\tilde{u}_j)}{\partial x_j} = -\frac{\partial \bar{p}}{\partial x_i} + \frac{\partial}{\partial x_j}\left[\left(\frac{\mu}{Re} + \mu_{sgs} \right)\left(2\tilde{S}_{ij} - \frac{2}{3}\frac{\partial \tilde{u}_k}{\partial x_k}\delta_{ij} \right) \right] + \frac{1}{Fr^2}\bar{\rho} g_i \tag{5}$$

$$Mr^2 \left[\frac{\partial}{\partial t}\left(\bar{p} + \frac{\gamma-1}{2}\bar{\rho}\tilde{u}_i\tilde{u}_i \right) + \frac{\partial}{\partial x_j}\left(\gamma\bar{p} + \frac{\gamma-1}{2}\bar{\rho}\tilde{u}_i\tilde{u}_i \right)\tilde{u}_j \right] + \frac{\partial \tilde{u}_j}{\partial x_j} = \tag{6}$$

$$(\gamma-1)Mr^2\frac{\partial}{\partial x_j}\left[\left(\frac{\mu}{Re} + \mu_{sgs} \right)\left(2\tilde{S}_{ij} - \frac{2}{3}\frac{\partial \tilde{u}_k}{\partial x_k}\delta_{ij} \right)\tilde{u}_i \right] + \frac{\partial}{\partial x_j}\left[\left(\frac{\mu}{RePr} + \frac{\mu_{sgs}}{Pr_{sgs}} \right)\frac{\partial \widetilde{T}}{\partial x_j} \right] + \frac{Ec}{Fr^2}(\bar{\rho}\tilde{u}_i g_i) \tag{7}$$

Note that the eddy viscosity assumption for the SGS stress term and eddy-diffusivity hypothesis for the SGS heat flux term are used together with some assumptions to discard the terms negligibly small below the hypersonic regime.

4 SGS Modeling

Linear eddy-viscosity SGS models have the following general form for the SGS dynamic viscosity,

$$\mu_{sgs} = \bar{\rho}(C_m\Delta)^2 \ \overline{DO(\vec{x},t)} \tag{8}$$

where C_m is the model coefficient, Δ is the length scale and $\overline{DO(\vec{x},t)}$ is the time- and space-dependent differential operator usually built on the resolved velocity field. For example, the eddy-viscosity in the Smagorinsky model is written as

$$\mu_{sgs} = \bar{\rho}(C_m\Delta)^2 \ \overline{DO(\vec{x},t)} \tag{9}$$

Here, $\overline{DO(\vec{x},t)}$ is given in terms of the magnitude of the strain-rate tensor, $|\bar{S}| = (2\bar{S}_{ij}\bar{S}_{ij})^{1/2}$.

Eidson[2] modified the differential operator to account for the buoyancy effects. The derivation was based on the two assumptions. The first one assumes that buoyancy contributes to the SGS production P_{sgs} through SGS heat flux term $v'T'$ in a specified direction. It is also scaled by a coefficient obtained from the non-dimensional form of the governing equations with the Boussinesq approximation. The second

one assumes that SGS dissipation ε and P_{sgs} are in equilibrium. Then, the buoyancy-modified Smagorinsky model was obtained in the general notation as

$$\mu_{sgs} = \bar{\rho}(C_s\Delta)^2 \left[\overline{DO(\vec{x},t)}^2 + Buoyancy\right]^{1/2} \tag{10}$$

It is written explicitly in dimensional form as

$$\mu_{sgs} = \bar{\rho}(C_s\Delta)^2 \left(|\bar{S}|^2 + \frac{\beta}{Pr_{sgs}}\frac{\partial\tilde{T}}{\partial x_j}g_k\delta_{kj}\right)^{1/2} \tag{11}$$

or in non-dimensional form

$$\mu_{sgs} = \bar{\rho}(C_s\Delta)^2 \left(|\bar{S}|^2 - \frac{PrRa}{Pr_{sgs}}\frac{\partial\tilde{T}}{\partial x_j}\delta_{2j}\right)^{1/2} \tag{12}$$

For further details of the derivation, see [2].

Two other variants were also developed. Peng and Davidson[5] suggested another scaling to obtain numerically more stable version which can be written in dimensional form as

$$\mu_{sgs} = \bar{\rho}(C_s\Delta)^2\frac{1}{|\bar{S}|}\left(|\bar{S}|^2 - \frac{g\beta}{Pr_{sgs}}\frac{\partial\tilde{T}}{\partial x_j}\delta_{2j}\right) \tag{13}$$

Worthy and Rubini[8] was also reformulated to remove the low-Mach number restriction which reads

$$\mu_{sgs} = \bar{\rho}(C_s\Delta)^2\left(|\bar{S}|^2 + B_{corr}\right)\bar{S}_{ij}^2 + B \tag{14}$$

where B is the buoyancy contribution and B_{corr} is the compressibility correction term for buoyancy. However, both have the well-known pitfalls of the classical Smagorinsky model such as excessive dissipation, near-wall correction, etc. that limits the application areas.

Obtaining numerically robust and efficient SGS model for buoyant flows with heat transfer is still an active research area in literature. Transitional and/or turbulent wall-bounded flows obviously have rich physical structures and require detailed studies to identify and characterize the effects of buoyancy and heat transfer. Moving from that point, it is motivated to propose an effective approach especially addresses to scaling over-dissipation and improving near-wall behavior.

The classical WALE model is chosen as the base SGS model for this purpose. It is an advanced, algebraic eddy-viscosity model. It utilizes a differential operator based on the traceless symmetric part of the square of the velocity gradient tensor

$$S_{ij}^d = \frac{1}{2}(\tilde{g}_{ij}^2 + \tilde{g}_{ji}^2) - \frac{1}{3}\delta_{ij}\tilde{g}_{kk}^2 \tag{15}$$

where $\tilde{g}_{ji}^2 = \tilde{g}_{ik}\tilde{g}_{kj}$ and $\tilde{g}_{kj}$ is the velocity gradient tensor, and calculates μ_{sgs} using

$$\mu_{sgs} = \bar{\rho}(C_W\Delta)^2\ \overline{DO(\vec{x},t)} \tag{16}$$

where

$$\overline{DO(\vec{x},t)} = \frac{(S_{ij}^dS_{ij}^d)^{3/2}}{(\widetilde{S}_{ij}\widetilde{S}_{ij})^{5/2} + (S_{ij}^dS_{ij}^d)^{5/4}} \tag{17}$$

and $C_W = \sqrt{10.6}C_{sma}$ where C_{sma} is the Smagorinsky constant. $C_{sma} = 0.1$ gives $C_W \approx 0.33$.

Applying the ideas of Eidson and following the same derivation procedure, the SGS viscosity based on the proposed BM-WALE model takes the following non-dimensional explicit form

$$\mu_{sgs} = \bar{\rho}(C_W\Delta)^2\left(\left(\frac{(S_{ij}^dS_{ij}^d)^{3/2}}{(\widetilde{S}_{ij}\widetilde{S}_{ij})^{5/2} + (S_{ij}^dS_{ij}^d)^{5/4}}\right)^2 + \frac{1}{Fr^2Pr_{sgs}}\frac{\partial\widetilde{T}}{\partial x_j}\delta_{2j}\right)^{1/2} \tag{18}$$

Note that, the scaling coefficient $\frac{1}{Fr^2}$ comes from the Eq.5. Pr_{sgs} was taken as 0.8 in this study.

The proposed model exhibits the advanced features of the WALE model. It performs well near walls, scales its inherent SGS dissipation contribution for shear or transitional flows, and more importantly recovers its original version for isothermal flows.

5 Solver

An in-house, fully implicit, fully parallel LES solver, *i*LES, based on the numerical method in Sec. 2 is used. It is written based on the object-oriented PETSc library[9] using Fortran syntax. Distributed array context in PETSc is used for data management. *i*LES was also modified to introduce the proposed SGS modeling approach.

6 Results and Discussions

RBC occurs when a horizontal layer of fluid between plates is heated from below and cooled from above. It is an example of thermally- and buoyancy-driven instability. Many natural and industrial flows can be given as examples such as solar interiors, atmospheric flows, cooling nuclear reactors, fire, combustion, etc.

The Rayleigh number is a primary dimensionless quantity when defining RBC. It determines whether the convective regime is laminar or turbulent, or if it is turbulent, whether it is soft or hard. The Rayleigh number is written as

$$Ra = \frac{\rho g \beta \Delta T H^3}{\mu \kappa} \tag{19}$$

where β and κ are the thermal expansion and thermal diffusivity coefficients respectively. When the temperature difference ΔT is sufficiently large, this leads to high Rayleigh number and the instability evolves into the turbulent state. When $\beta \Delta T \geq 0.1 - 0.15$, the Boussinessq assumption is no more valid [10].

The soft turbulent regime is studied here. The working fluid is air. The Rayleigh number is $Ra = 6.3 \times 10^5$ with $\Delta T = 30^\circ K$. Note that this temperature difference is within the validity range of the Boussinessq assumption and corresponds to the upper limit for air. The initial fields are

$$u, v, w = 0 \tag{20}$$

$$\rho = \rho_0 (1 + \beta (\frac{\Delta T}{H}) y) \tag{21}$$

$$p = p_0 - \rho g y \tag{22}$$

$$T = T_0 - (\frac{\Delta T}{H}) y \tag{23}$$

The stream-wise (x) and the span-wise(z) boundary conditions are periodic. The normal-wise(y) boundary contitions are defined as no-slip walls. The domain aspect ratio is 6. The grid is uniform Cartesian with $64 \times 96 \times 64$ resolution. Note that, for this Rayleigh number, the Kolmogorov length scale can be estimated via

$$\frac{\eta}{H} = \frac{\sqrt{Pr}}{[(Nu - 1) Ra]^{\frac{1}{4}}} \tag{24}$$

and gives ≈ 0.0188. The vertical grid resolution is $\Delta y = 0.0104$ in this simulation and sufficiently satisfies the Kolmogorov estimation. In fact, unlike the many other RBC study, the same resolution is used for the interiors. For LES, the minimum grid spacing can be found via [11]

$$\frac{\lambda}{H} = \frac{\sqrt{15} \sqrt{0.0027 Ra^{1.04} + 0.0312 Ra^{0.92}}}{[(Nu - 1) Ra]^{\frac{1}{2}}} \tag{25}$$

that gives 0.1342. Again, the horizontal grid spacings $\Delta x = \Delta z = 0.09375$ are fairly sufficient in the present simulation. The approximate thermal boundary layer thickness can be computed as $\frac{\lambda_T}{H} = \frac{1}{2Nu} = 0.0676$. In this case, the thermal boundary layers are resolved by at least $6 - 7$ cells. Higher Rayleigh numbers

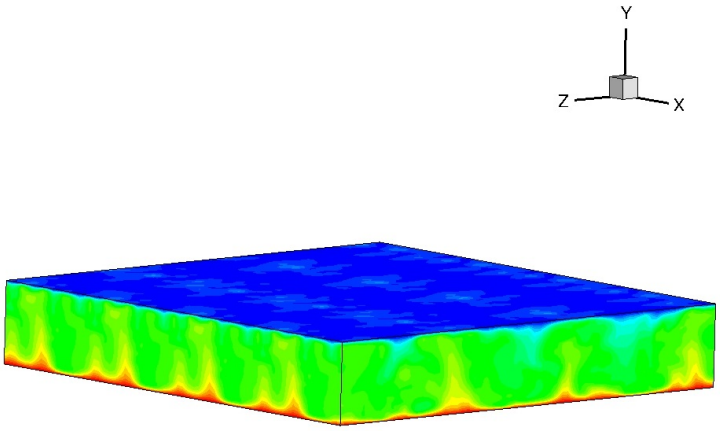

Figure 1: The instantaneous temperature field at $1350\tau_c$

require finer resolutions and more cells to properly resolve the boundary layers. The above calculations use $Nu = 0.186Ra^{0.276}$ relation taken from a DNS study[12].

The extent of the domain H, $u_c = \sqrt{g\beta\Delta TH}$ and $\tau_c = \frac{H}{u_c}$ are the reference length, convective velocity and the convective time respectively. The evolution of the instability was followed up to a sufficiently long time ($2100\tau_c$) to obtain correct statistics which were collected at least during the last one-third of the simulation [13]. The turbulent statistics are computed as

$$\phi' = \phi - \langle\phi\rangle \tag{26}$$

$$\phi_{rms} = (\langle\phi'^2\rangle)^{\frac{1}{2}} \tag{27}$$

Note that the $\langle\ \rangle$ symbol used above also includes the time-averaging in addition to the averaging over the horizontal directions.

Fig.1 shows the instantaneous temperature field at $1350\tau_c$. The large scale coherent motions of upward and downward plumes are clearly seen.

The vertical distributions of the average temperature and the *rms* of its fluctuations are plotted in Fig.2 and Fig.3 respectively. The result of the WALE SGS model is also provided for comparison. Both models behave similarly and their results are successfully compared with the previously reported experimental and numerical data [4, 11, 14, 15]. The peak values of the thermal fluctuations near walls are computed slightly larger. However, the thermal boundary layer thicknesses are predicted well. The value of the T_{rms} in interior region is the least one among the data presented, but still in the range. Note that the present LES simulation resolves the inner region again by using a grid finer than that of the other numerical data in the figure and uses no stretching.

The *rms* of the vertical velocity fluctuations and its skewness

$$S_{v'} = \frac{\langle v'^3\rangle}{\langle v'^2\rangle^{\frac{3}{2}}} \tag{28}$$

are shown in Fig.4 and Fig.5 respectively. Both the WALE and the BM-WALE models predict the distribution sufficiently well. There is no significant difference between them.

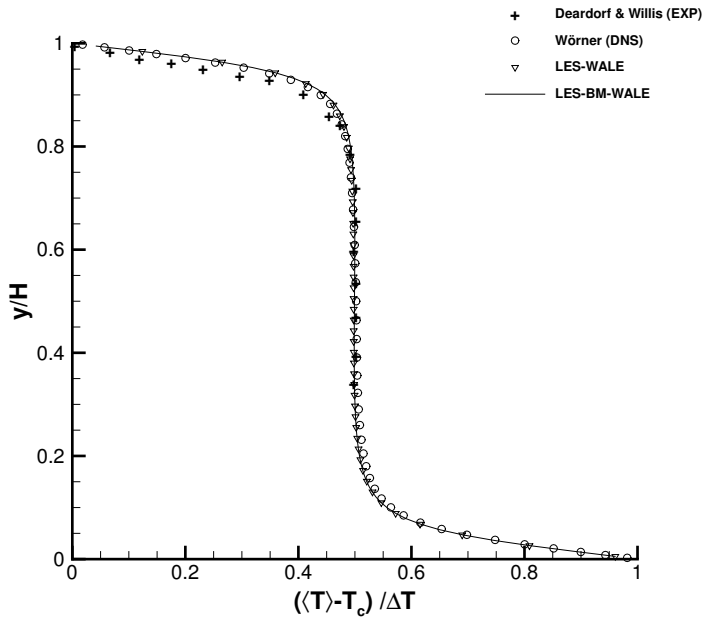

Figure 2: Vertical distribution of the average temperature

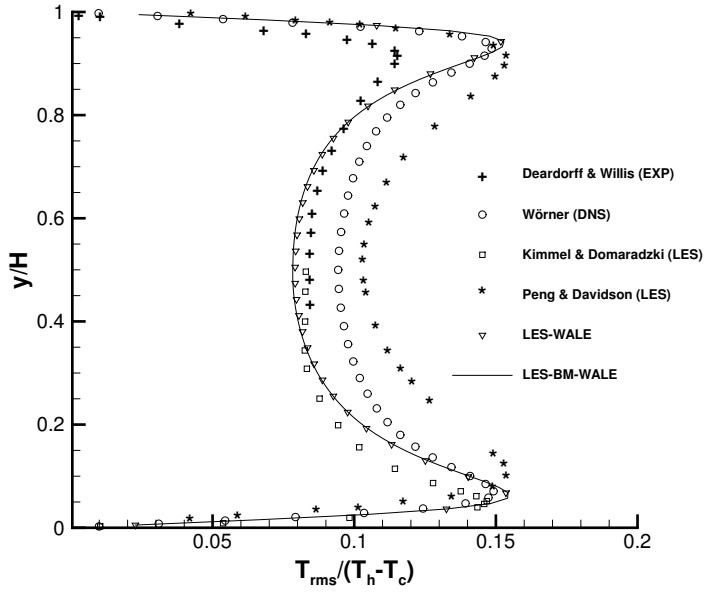

Figure 3: Vertical distribution of *rms* of the temperature fluctuations

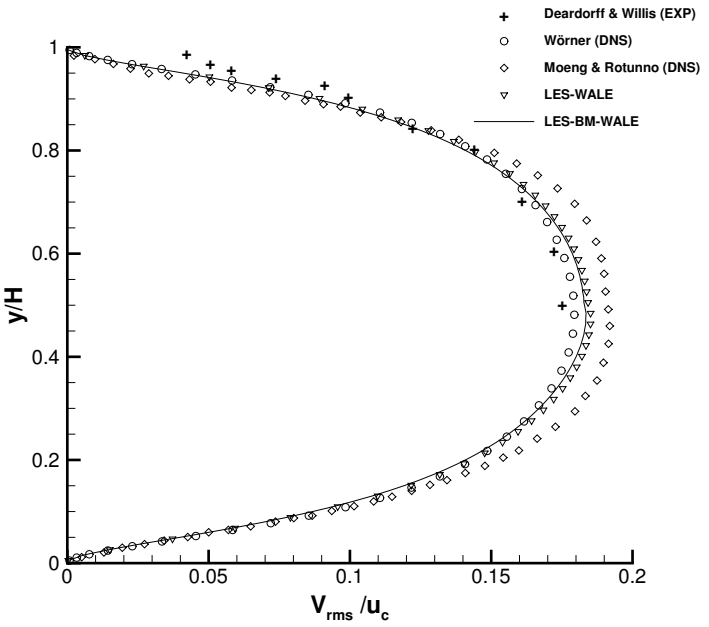

Figure 4: Vertical distribution of *rms* of the vertical velocity fluctuations

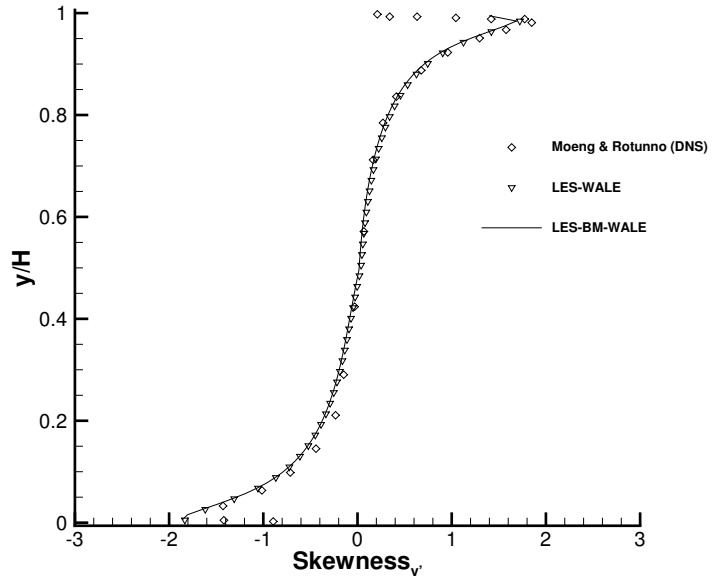

Figure 5: Skewness of the vertical velocity fluctuation

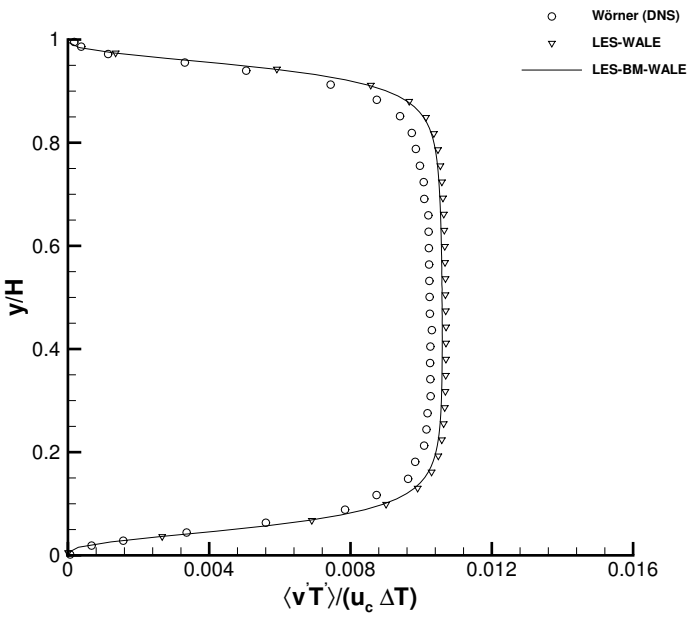

Figure 6: The vertical distribution of $< v'T' >$

The turbulent heat flux $< v'T' >$ is given in Fig.6. As expected, it goes to zero toward walls. Its distribution is predicted slightly less than The WALE model around the center, but closer to DNS.

Then, the Nusselt number was computed according to formula

$$Nu(y) = \frac{< v'T' > - < \kappa \partial T/\partial y >}{\kappa \Delta T/H} \tag{29}$$

and its vertical distribution is plotted in Fig.7. The integrated Nu value is well predicted as 7.17. The WALE model gives 7.22. The negligible difference between them is due to the smaller prediction of $< v'T' >$ in the inner region. Jumps observed near walls are possibly due to large temperature gradients. Finer grid resolutions or long simulation/sampling times can be used to get more uniform distribution.

Finally, Fig.8 gives the turbulent kinetic energy, k, distribution. Near wall region is consistent with the DNS data. However, k is under-estimated around center. Again, DNS data was obtained using a stretched mesh which is finer near walls and coarser around center, whereas the present simulation resolves everywhere in the domain almost by the half the Kolmogorov length scale without stretching. It is possible that the coarse-DNS over-estimates the distribution of k with a wavy pattern.

7 Conclusion and Future Work

A SGS model for LES of transitional and turbulent flows which takes the effects of buoyancy for under-resolved scales was proposed and applied to the challenging turbulent Rayleigh-Bénard convection. These preliminary results show that the proposed model is very promising approach and is capable of handling the overall physics of buoyant convection problem accurately. It does not disrupt the well-known behavior of the WALE model, instead the results are enhanced and relatively better results are obtained for especially the quantities related to turbulent heat transfer compared with the original one. For flows with $\frac{\partial \widetilde{T}}{\partial x_j}\delta_{2j} = 0$, it reverts to the classical WALE.

Further analyses and applications with more diagnostics are obviously required to characterize the behavior of the proposed model.

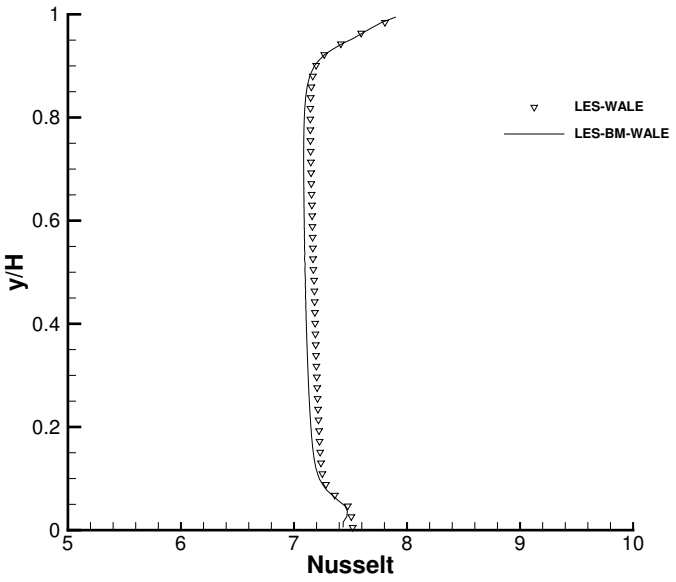

Figure 7: The vertical distribution of Nu

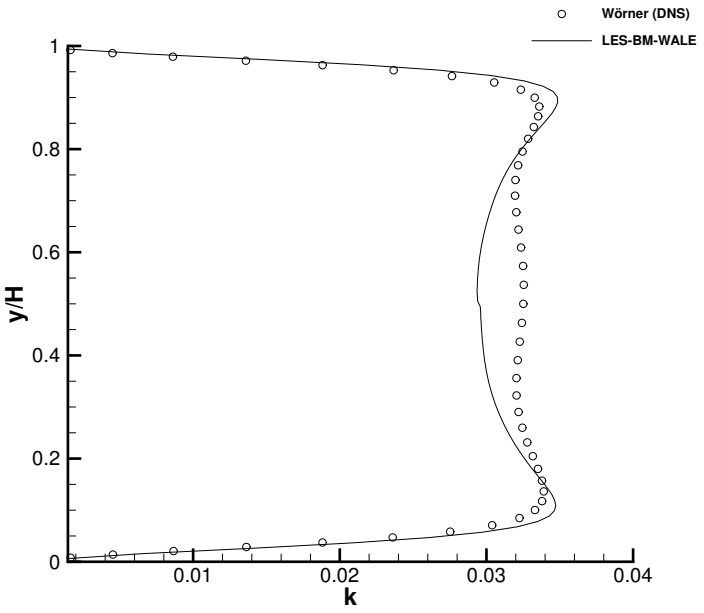

Figure 8: The vertical distribution of turbulent kinetic energy

References

[1] D. K. Lily. On the numerical simulation of buoyant convection. *Tellus*, 14(2):148–172, 1962.

[2] T. M. Eidson. Numerical simulation of the turbulent Rayleigh-Bénard problem using subgrid modelling. *Journal of Fluid Mechanics*, 158:245–268, 9 1985.

[3] R. J. M. Bastiaans, C. C. M. Rindt, F. T. M. Nieuwstadt, and A. A. van Steenhoven. Direct and large-eddy simulation of the transition of two- and three-dimensional plane plumes in a confined enclosure. *International Journal of Heat and Mass Transfer*, 43(13):2375 – 2393, 2000.

[4] S. J. Kimmel and J. A. Domaradzki. Large eddy simulations of Rayleigh-Bénard convection using subgrid scale estimation model. *Physics of Fluids*, 12(1), 2000.

[5] S.-H. Peng and L. Davidson. Numerical investigation of turbulent buoyant flow in a cavity using large eddy simulation. In *Turbulence Heat and Mass Transfer 3/Nagano, Y., Hanjalic, K., Tsuji, T.*, pages 737–744, 2000.

[6] F. Nicoud and F. Ducros. Subgrid-scale stress modelling based on the square of the velocity gradient tensor. *Flow, Turbulence and Combustion*, 62:183–200, 1999.

[7] Y. Hou and K. Mahesh. A robust, colocated, implicit algorithm for direct numerical simulation of compressible, turbulent flows. *J. Comput. Phys.*, 205:205–221, 2005.

[8] Worthy J. and Rubini P. A study of LES stress and flux models applied to a buoyant jet. *Numerical Heat Transfer Part B: Fundamentals*, 48(3):235–256, 2005.

[9] Satish Balay, William D. Gropp, Lois C. McInnes, and Barry F. Smith. Efficienct management of parallelism in object oriented numerical software libraries. In E. Arge, A. M. Bruaset, and H. P. Langtangen, editors, *Modern Software Tools in Scientific Computing*, page 163âĂŞ202. Birkhauser Press, 1997.

[10] Gray D.D. and Giorgini A. The validity of the Boussinesq approximation for liquids and gases. *Int. J. of Heat and Mass Transfer*, 19(5):545–551, 1976.

[11] S-H. Peng, L. Davidson, and K. Hanjalic. Numerical analysis of Rayleigh–Bénard convection flow using large eddy simulation at high rayleigh numbers. *Proc. of The Fourth Int. Symp. on Turbulence and Shear Flow Phenomena*, 3:983–988, 2005.

[12] R.M. Kerr. Rayleigh number scaling in numerical convection. *J. Fluid Mech.*, 310:139–179, 1976.

[13] G. Silano, K.R. Sreenivasan, and R. Verzicco. Numerical simulations of Rayleigh-Bénard convection for prandtl numbers between 10^{-1} and 10^4 and Rayleigh numbers between 10^5 and 10^9. *J. Fluid Mech.*, 662:409–446, 2010.

[14] J.W. Deardorff and G.E. Willis. Investigation of turbulent thermal convection between horizontal plates. *J. Fluid Mech.*, 28:675–704, 1967.

[15] M. Wörner. Direkte simulation turbulenter rayleigh-bénard konvektion in fluessigem natrium. *PhD Thesis, University of Karlsruhe*, 1994.